Boundary-Layer Meteorol (2014) 153:327–337
DOI 10.1007/s10546-014-9947-x

RESEARCH NOTE

Towards a Flux-Partitioning Procedure Based on the Direct Use of High-Frequency Eddy-Covariance Data

Luigi Palatella · Gianfranco Rana · Domenico Vitale

Received: 31 October 2013 / Accepted: 17 June 2014 / Published online: 6 July 2014

Abstract Scanlon and Sahu (Water Resour Res 44(10):W10418, 2008) proposed an interesting method to estimate assimilation, respiration, evaporation and transpiration directly using high-frequency eddy-covariance measurements. In this note we critically revise this method and, in particular, using the Descartes' rule of sign, we show that one branch of solutions can be directly neglected reducing the analytical complexity of the procedure. We also discuss the stability of the results of the method with respect to the input parameters, especially to the water-use efficiency.

Keywords Evaporation · Photosynthesis · Respiration · Transpiration · Water-use efficiency

1 Introduction

Carbon dioxide (CO_2) and water vapour (H_2O) fluxes are currently measured through several networks of eddy-covariance (EC) stations around the world Baldocchi et al. (2001). The EC technique is based on high-frequency (10–20 Hz) measurements of wind velocity as

L. Palatella (✉)
ISAC-CNR, Istituto di Scienze dell'Atmosfera e del Clima, U.O.S. di Lecce,
Str. Prov. Lecce-Monteroni km 1,200, Lecce, Italy
e-mail: luigi.palatella@yahoo.it

L. Palatella
INFN sez. Lecce, Lecce, Italy

G. Rana
CRA-SCA, Consiglio per la Ricerca e la Sperimentazione in Agricoltura, Unità di Ricerca per i Sistemi Colturali degli Ambienti Caldo-Aridi, via C. Ulpiani 5, Bari, Italy

D. Vitale
DIBAF, Dipartimento per l'Innovazione nei sistemi Biologici, Agroalimentari e Forestali,
University of Tuscia, via C. de Lellis, 01100 Viterbo, Italy

well as CO_2 and H_2O concentrations at a point over the canopy using a three-axis sonic anemometer and a fast response infrared gas analyzer. Assuming perfect turbulent mixing, these measurements are typically averaged over periods of 0.5–1 h, forming the basis of calculating carbon and water balances from daily to annual time scales.

For the purpose of ecosystem studies and modelling, the calculated fluxes from EC data need to be partitioned into their main components: evaporation and transpiration for water vapour and photosynthesis and respiration for carbon dioxide. There are several methods to reach this target (see Reichstein et al. 2012 for more details and references). The standard approaches (i.e. those used in FLUXNET) are based on the use of only filtered nighttime data to directly measure the respiration flux (Reichstein et al. 2005). Other methods use both daytime and nighttime data or only daytime data, using light response curves (Lasslop et al. 2010). Both methods are combined to obtain the partition of net ecosystem exchange of CO_2 (NEE) into gross primary production (GPP) and ecosystem respiration (R_{eco}).

A challenge in partitioning is the estimate of assimilation and respiration using only high-frequency EC measurements as proposed recently by Scanlon and Sahu (2008) (hereafter called SS08) and Scanlon and Kustas (2010). This approach is based on the argument that the high-frequency flux data contain more information about the source of fluxes and assimilation respiration dynamics than is commonly acknowledged. SS08 applied flux-variance Monin-Obukhov similarity theory (MOST) separately to the stomatal (i.e. photosynthesis and transpiration) and non-stomatal processes. They provided an analytical expression based on the leaf-level water-use efficiency (W) for a given crop to partition both carbon dioxide (F_c) and water vapour (F_q) fluxes. Therefore, it should be sufficient to measure CO_2 and H_2O concentrations in order to have the partitioned fluxes at the same time scale.

To our knowledge, despite this method seeming very promising, it has been scarcely used for practical application up to now (Reichstein et al. 2012). The reasons may be related to the computational complexity or to the awkwardness of some mathematical steps in its realization. In this note we report a critical revision of the method proposed by SS08 in order to stress the critical points and to increase the practical applicability of the method.

2 The Proposal of Scanlon and Sahu (2008)

Let us start with several definitions: the fluctuations of the water vapour (q') and carbon dioxide (c') scalar atmospheric concentrations measured over the crop can be partitioned into transpiration (q'_{t}), evaporation (q'_{e}), photosynthesis (c'_{p}) and respiration (c'_{r}) components resulting in the following

$$c' = c'_{\mathrm{p}} + c'_{\mathrm{r}}, \tag{1}$$

$$q' = q'_{\mathrm{t}} + q'_{\mathrm{e}}. \tag{2}$$

The q'_{t} and c'_{p} components are linked to the water-use efficiency (W) of the crop under examination by

$$c'_{\mathrm{p}} = W\, q'_{\mathrm{t}}. \tag{3}$$

Notice that with this definition we have $W < 0$. Let $\sigma_{q'_{\mathrm{t}}}$, $\sigma_{q'_{\mathrm{e}}}$, $\sigma_{c'_{\mathrm{p}}}$, $\sigma_{c'_{\mathrm{r}}}$ be the associated standard deviations given by $\sigma_{q'_{\mathrm{e}}} = \langle q'^2_{\mathrm{e}} \rangle^{1/2}$, $\sigma_{c'_{\mathrm{r}}} = \langle c'^2_{\mathrm{r}} \rangle^{1/2}$, $\sigma_{q'_{\mathrm{t}}} = \langle q'^2_{\mathrm{t}} \rangle^{1/2}$, $\sigma_{c'_{\mathrm{p}}} = \langle c'^2_{\mathrm{p}} \rangle^{1/2}$, where $\langle \cdot \rangle$ denotes the time averaging over a time interval of 0.5–1 h. Then we have

$$\sigma_{c'_\mathrm{p}} = -W\,\sigma_{q'_\mathrm{t}}, \tag{4}$$

$$\sigma^2_{c'_\mathrm{p}} = W^2\sigma^2_{q'_\mathrm{t}}. \tag{5}$$

The same approach can be used to partition turbulent fluxes (without the density terms)

$$F_q = \langle w'q'\rangle = \langle w'q'_\mathrm{t}\rangle + \langle w'q'_\mathrm{e}\rangle, \tag{6}$$

$$F_\mathrm{c} = \langle w'c'\rangle = \langle w'c'_\mathrm{p}\rangle + \langle w'c'_\mathrm{r}\rangle = W\langle w'q'_\mathrm{t}\rangle + \langle w'c'_\mathrm{r}\rangle, \tag{7}$$

where w' is the vertical velocity fluctuation and, as before, $\langle\cdot\rangle$ stands for the time-averaging procedure over a time interval of 0.5–1 h.

At this point, SS08 introduced the main approximations of the whole method, namely

$$\rho_{q'_\mathrm{t},q'_\mathrm{e}} \equiv \frac{\langle q'_\mathrm{t}q'_\mathrm{e}\rangle}{\sigma_{q'_\mathrm{t}}\sigma_{q'_\mathrm{e}}} \simeq \frac{\rho_{w',q'_\mathrm{e}}}{\rho_{w',q'_\mathrm{t}}} = \frac{\langle w'q'_\mathrm{e}\rangle}{\langle w'q'_\mathrm{t}\rangle}\frac{\sigma_{q'_\mathrm{t}}}{\sigma_{q'_\mathrm{e}}}, \tag{8}$$

$$\rho_{c'_\mathrm{p},c'_\mathrm{r}} \equiv \frac{\langle c'_\mathrm{p}c'_\mathrm{r}\rangle}{\sigma_{c'_\mathrm{p}}\sigma_{c'_\mathrm{r}}} \simeq \frac{\rho_{w',c'_\mathrm{r}}}{\rho_{w',c'_\mathrm{p}}} = \frac{\langle w'c'_\mathrm{r}\rangle}{\langle w'c'_\mathrm{p}\rangle}\frac{\sigma_{c'_\mathrm{p}}}{\sigma_{c'_\mathrm{r}}}. \tag{9}$$

These approximations are proposed and discussed in Katul et al. (1995, 1996) and Bink and Meesters (1997). The physical mechanism underlying the definition of the different fluxes allows us to obtain the correlation between their components, namely

$$\rho_{q'_\mathrm{t},c'_\mathrm{p}} = -1, \tag{10}$$

$$\rho_{q'_\mathrm{e},c'_\mathrm{r}} = +1, \tag{11}$$

$$\rho_{q'_\mathrm{t},q'_\mathrm{e}} = -\rho_{c'_\mathrm{p},c'_\mathrm{r}}. \tag{12}$$

Following SS08, the variances of q' and c' are defined as

$$\sigma^2_{q'} = \sigma^2_{q'_\mathrm{t}} + \sigma^2_{q'_\mathrm{e}} + 2\rho_{q'_\mathrm{t},q'_\mathrm{e}}\sigma_{q'_\mathrm{t}}\sigma_{q'_\mathrm{e}}, \tag{13}$$

$$\sigma^2_{c'} = \sigma^2_{c'_\mathrm{p}} + \sigma^2_{c'_\mathrm{r}} + 2\rho_{c'_\mathrm{p},c'_\mathrm{r}}\sigma_{c'_\mathrm{p}}\sigma_{c'_\mathrm{r}}, \tag{14}$$

which, by substituting from Eqs. 5, 8 and 9, become

$$\sigma^2_{q'} = \frac{1}{W^2}\sigma^2_{c'_\mathrm{p}} + \left[\frac{\langle w'q'_\mathrm{e}\rangle}{\langle w'q'_\mathrm{t}\rangle}\right]^2\frac{\sigma^2_{c'_\mathrm{p}}}{W^2\rho^2_{c'_\mathrm{p},c'_\mathrm{r}}} + 2\frac{\sigma^2_{c'_\mathrm{p}}}{W^2}\frac{\langle w'q'_\mathrm{e}\rangle}{\langle w'q'_\mathrm{t}\rangle}, \tag{15}$$

$$\sigma^2_{c'} = \sigma^2_{c'_\mathrm{p}} + \left[\frac{\langle w'c'_\mathrm{r}\rangle}{\langle w'c'_\mathrm{p}\rangle}\right]^2\frac{\sigma^2_{c'_\mathrm{p}}}{\rho^2_{c'_\mathrm{p},c'_\mathrm{r}}} + 2\sigma^2_{c'_\mathrm{p}}\frac{\langle w'c'_\mathrm{r}\rangle}{\langle w'c'_\mathrm{p}\rangle}. \tag{16}$$

Defining $\tilde{q} \equiv \frac{\langle w'q'_\mathrm{e}\rangle}{\langle w'q'_\mathrm{t}\rangle}$ and $\tilde{c} \equiv \frac{\langle w'c'_\mathrm{r}\rangle}{\langle w'c'_\mathrm{p}\rangle}$, Eqs. 15 and 16 can be written, respectively, as

$$\frac{\tilde{q}^2}{\rho^2_{c'_\mathrm{p},c'_\mathrm{r}}} + 2\tilde{q} + 1 - \left(\frac{\sigma_{q'}W}{\sigma_{c'_\mathrm{p}}}\right)^2 = 0, \tag{17}$$

$$\frac{\tilde{c}^2}{\rho^2_{c'_\mathrm{p},c'_\mathrm{r}}} + 2\tilde{c} + 1 - \left(\frac{\sigma_{c'}}{\sigma_{c'_\mathrm{p}}}\right)^2 = 0, \tag{18}$$

which are both in quadratic form. By rearranging Eqs. 6 and 7, we obtain respectively

$$\langle w' q_{\mathrm{t}}' \rangle = \frac{\langle w' q' \rangle}{1 + \tilde{q}_{\pm}}, \tag{19}$$

$$\langle w' c_{\mathrm{p}}' \rangle = \frac{\langle w' c' \rangle}{1 + \tilde{c}_{\pm}}, \tag{20}$$

where the subscript $\pm$ denotes one of the two possible solutions resulting from the quadratic forms. Since $W = \frac{\langle w' c_{\mathrm{p}}' \rangle}{\langle w' q_{\mathrm{t}}' \rangle}$, by substituting from Eqs. 19 and 20 we obtain

$$W = \frac{\langle w' c' \rangle}{\langle w' q' \rangle} \frac{1 + \tilde{q}_{\pm}}{1 + \tilde{c}_{\pm}}, \tag{21}$$

which is equivalent to Eq. 15 reported in SS08, and where W, $\rho_{c_{\mathrm{p}}', c_{\mathrm{r}}'}$ and $\sigma_{c_{\mathrm{p}}'}$ are the only variables that are not directly measured by eddy correlation. By Eq. 21, given an estimate of the W, we are able to establish the relationships between $\rho_{c_{\mathrm{p}}', c_{\mathrm{r}}'}$ and $\sigma_{c_{\mathrm{p}}'}$, in particular confining $\rho_{c_{\mathrm{p}}', c_{\mathrm{r}}'}$ to the physically meaningful range $-1 \leq \rho_{c_{\mathrm{p}}', c_{\mathrm{r}}'} \leq 0$. For each pair of values, it is therefore possible to solve Eqs. 17 and 18 and to find the individual flux components from Eqs. 19 and 20. Only physically meaningful values of these components are considered (i.e. $\langle w' q_{\mathrm{t}}' \rangle \geq 0$, $\langle w' q_{\mathrm{e}}' \rangle \geq 0$, $\langle w' c_{\mathrm{p}}' \rangle \leq 0$, $\langle w' c_{\mathrm{r}}' \rangle \geq 0$).

Since Eq. 21 has two unknowns, to solve the system another equation is needed. This can be obtained by requiring that the calculated correlation between q' and c' scalars, $\rho_{q',c'}$, is equal to the correlation obtained from the experimental data $\rho^{\mathrm{obs}}_{q',c'}$. We thus have

$$\rho^{\mathrm{obs}}_{q',c'} = \frac{1}{\sigma_{c'} \sigma_{q'}} \left\{ \frac{\sigma^2_{c_{\mathrm{p}}'}}{W} + \rho_{c_{\mathrm{p}}', c_{\mathrm{r}}'} \sigma_{c_{\mathrm{p}}'} \sigma_{c_{\mathrm{r}}'} \left(\frac{1}{W} + \frac{\langle w' q_{\mathrm{e}}' \rangle}{\langle w' c_{\mathrm{r}}' \rangle} \right) + \sigma^2_{c_{\mathrm{r}}'} \frac{\langle w' q_{\mathrm{e}}' \rangle}{\langle w' c_{\mathrm{r}}' \rangle} \right\} \tag{22}$$

where $\sigma_{c_{\mathrm{r}}'}$ can be estimated from Eq. 9 as a function of $\sigma_{c_{\mathrm{p}}'}$ and $\rho_{c_{\mathrm{p}}', c_{\mathrm{r}}'}$. When $\rho^{\mathrm{obs}}_{q',c'}$ does not match $\rho_{q',c'}$, SS08 proposed a wavelet filtering procedure in order to remove large-scale factors such as entrainment or non-stationarity that potentially influence the time series statistics (see SS08 for more details).

3 Solution Methods

Equations 21 and 22 constitute a closed system in two unknowns parameters $\rho_{c_{\mathrm{p}}', c_{\mathrm{r}}'}$ and $\sigma_{c_{\mathrm{p}}'}$ to be solved, constrained to the conditions

$$-1 \leq \rho_{c_{\mathrm{p}}', c_{\mathrm{r}}'} \leq 0, \tag{23a}$$

$$\sigma_{c_{\mathrm{p}}'} \geq 0. \tag{23b}$$

3.1 Specific Constraints for Eq. 17

Let us start with the constraint related to the discriminant (Δ) of the quadratic Eq. 17 given by

$$\Delta_{(17)} \geq 0 \iff \sigma_{c_{\mathrm{p}}'} \leq -\frac{\sigma_{q'} W}{\sqrt{1 - \rho^2_{c_{\mathrm{p}}', c_{\mathrm{r}}'}}}. \tag{24}$$

Since we expect that the evaporation and transpiration water fluxes have the same sign, we are interested in the solutions fulfilling the condition $\tilde{q} \geq 0$. Making use of the Descartes' rule of sign, the only condition is that Eq. 17 should have one permanence and one variation

(so a negative and a positive root respectively). This condition is verified only if

$$\sigma_{c'_\mathrm{p}} \leq \sigma_{q'} \cdot |W| = -\sigma_{q'} W, \tag{25}$$

which is more restrictive than the $\Delta_{(17)}$ constraint. Thus, the condition $\tilde{q} \geq 0$ forces us to search for only one of the solutions of Eq. 17. In particular, looking for the positive one, we obtain

$$\tilde{q}_+ = \rho^2_{c'_\mathrm{p},c'_\mathrm{r}} \left\{ -1 + \sqrt{1 - \frac{1}{\rho^2_{c'_\mathrm{p},c'_\mathrm{r}}} \left[1 - \left(\frac{\sigma_{q'} W}{\sigma_{c'_\mathrm{p}}} \right)^2 \right]} \right\}. \tag{26}$$

3.2 Specific Constraints for Eq. 18

Since we expect that the related photosynthesis and respiration fluxes are of opposite sign, we are looking for $\tilde{c} \leq 0$. In this case the Descartes' rule of sign method does not help us to find physically meaningful solutions. In fact Eq. 18 could have two permanences (so two negative roots) if $\sigma_{c'_\mathrm{p}} \geq \sigma_c$ or one permanence and one variation (so only one negative root) if $\sigma_{c'_\mathrm{p}} \leq \sigma_c$. This implies solving (18) searching for both the solutions, that is

$$\tilde{c}_\pm = \rho^2_{c'_\mathrm{p},c'_\mathrm{r}} \left\{ -1 \pm \sqrt{1 - \frac{1}{\rho^2_{c'_\mathrm{p},c'_\mathrm{r}}} \left[1 - \left(\frac{\sigma_{c'}}{\sigma_{c'_\mathrm{p}}} \right)^2 \right]} \right\}. \tag{27}$$

Thus, the constraint related to (18) is the only one associated to its discriminant, namely

$$\Delta_{(18)} \geq 0 \iff \sigma_{c'_\mathrm{p}} \leq \frac{\sigma_{c'}}{\sqrt{1 - \rho^2_{c'_\mathrm{p},c'_\mathrm{r}}}} \tag{28}$$

3.3 General Constraints for Eq. 21

Given the specific constraints illustrated in the previous two sections, we can re-write Eq. 21 as

$$W = \frac{\langle w'c' \rangle}{\langle w'q' \rangle} \frac{1 + \tilde{q}_+}{1 + \tilde{c}_\pm}, \tag{29}$$

which can be solved subject to the constraints

$$-1 \leq \rho_{c'_\mathrm{p},c'_\mathrm{r}} \leq 0, \tag{30a}$$

$$0 \leq \sigma_{c'_\mathrm{p}} \leq \min \left[-\sigma_{q'} W, \quad \frac{\sigma_{c'}}{\sqrt{1 - \rho^2_{c'_\mathrm{p},c'_\mathrm{r}}}} \right]. \tag{30b}$$

3.4 The Numerical Scheme

Before showing details of the numerical implementation we now summarize the inputs and the outputs of the whole procedure. We start from the following measured or estimated inputs:

- $\sigma_{q'}$: the standard deviation of the water vapour concentration.
- $\sigma_{c'}$: the standard deviation of the CO_2 concentration.
- $\langle w'q' \rangle$: the eddy-covariance flux for water vapour.

– $\langle w'c' \rangle$: the eddy-covariance flux for CO_2.
– $\langle q'c' \rangle$: the eddy-covariance between water vapour and CO_2 concentration.
– W: the estimated water-use efficiency.

The numerical algorithm leads to the following main covariances:

– $\langle w'q'_{\rm e} \rangle$: the flux of evaporated water vapour.
– $\langle w'q'_{\rm t} \rangle$: the flux of transpired water vapour.
– $\langle w'c'_{\rm p} \rangle$: the flux of photosynthetic CO_2.
– $\langle w'c'_{\rm r} \rangle$: the flux of respirated CO_2.

In order to solve the non-linear system given by Eqs. 22 and 29 we propose a method slightly different from that proposed by SS08. As stated in Press et al. (1992), *there are no good, general methods for solving systems of more than one non-linear equation.* Of course this does not mean that the problem is not solvable, but that caution is needed when running numerical routines with different sets of parameters. The first problem is that the domain in the space $(\sigma_{c'_{\rm p}}, \rho_{c'_{\rm p},c'_{\rm r}})$ is not simply connected because all the constraints given in the previous sub-sections divide the domain into allowed and disallowed regions.

As explained in detail below, the routine we use to solve the nonlinear set of equations is based on the evaluation of the gradient of the mismatch between the two sides of the equations to be solved. Iterating the routine considered makes the consecutive estimates of the solution $\mathbf{x}$ moving in the plane $(\sigma_{c'_{\rm p}}, \rho_{c'_{\rm p},c'_{\rm r}})$ (like the red points in Fig. 1). This "trajectory" should converge to the solution point. This procedure becomes very difficult if some regions of the plane are forbidden due to the constraint given above. For this reason a non-connected domain (in other words a $(\sigma_{c'_{\rm p}}, \rho_{c'_{\rm p},c'_{\rm r}})$ plane with holes) represents a difficult problem for our algorithm. To this purpose we modify Eqs. 22 and 29 substituting the $\Delta_{(17)}$ and $\Delta_{(18)}$ with their absolute values and we neglect all the other constraints. We use the routine named *newt* and described as *globally convergent Newton's method* in Press et al. (1992). This routine is very fast and gives a very precise solution after less than ten steps. After the routine comes to convergence, we verify all the constraints on the solution obtained and if they are all fulfilled the solution is accepted.

Here we briefly outline the algorithm implemented in the routine *newt* given in Press et al. (1992). Solving a set of two non-linear equations with two unknowns x_1 and x_2 can be formally put in the form

$$F_i(\mathbf{x}) = 0, \tag{31}$$

where $i = 1, 2$ and $\mathbf{x} = (x_1, x_2)$. In the neighbourhood of $\mathbf{x}$, each of the functions F_i can be expanded in a Taylor series

$$F_i(\mathbf{x} + \delta\mathbf{x}) = F_i(\mathbf{x}) + \sum_{j=1}^{2} J_{ij}\delta x_j + O(\delta\mathbf{x}^2), \tag{32}$$

where the Jacobian matrix $\mathbf{J}$, with elements J_{ij}, is given by

$$J_{ij} = \frac{\partial F_i}{\partial x_j}. \tag{33}$$

In matrix notation we have

$$\mathbf{F}(\mathbf{x} + \delta\mathbf{x}) = \mathbf{F}(\mathbf{x}) + \mathbf{J}\delta\mathbf{x} + O(\delta\mathbf{x}^2) \tag{34}$$

and by neglecting terms of order $\delta\mathbf{x}^2$ and higher, and by setting $F(\mathbf{x} + \delta\mathbf{x}) = 0$, we obtain a set of linear equations for the corrections $\delta\mathbf{x}$ that move each function closer to zero simultaneously, namely

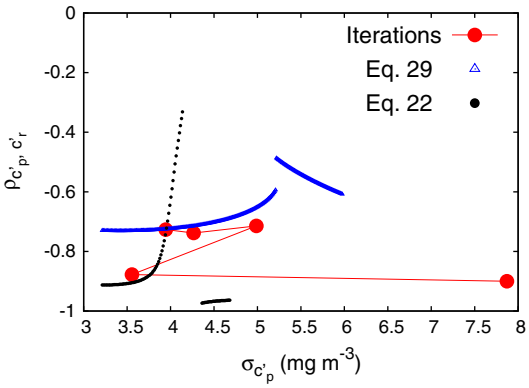

Fig. 1 Elaboration of the EC data obtained on April 7 2010 from 1300 to 1400 local time. The *red points* indicate the five iterations of the *newt* routine, the *blue* and *black points* represent one branch of the solutions of Eqs. 22 and 29, respectively

$$\mathbf{J} \cdot \delta\mathbf{x} = -F. \tag{35}$$

This equation is then solved using the LU decomposition Press et al. (1992). The corrections $\delta\mathbf{x}$ are then added to the solution vector

$$\mathbf{x}_{\text{new}} = \mathbf{x}_{\text{old}} + \delta\mathbf{x}, \tag{36}$$

and the process is iterated to convergence. In our case $\mathbf{J}$ is computed by a finite difference method.

Despite its efficiency the Newton method for solving non-linear equations has an unfortunate tendency to wander off if the initial guess is not sufficiently close to the root. A global method is one that converges to a solution from almost any starting point. The global algorithm *newt* is a modification of the bare Newton method according to the following procedure. If one defines the function

$$f \equiv \frac{1}{2}\mathbf{FF} \tag{37}$$

then the algorithm changes the value of the $\mathbf{x}$ estimate according to

$$\mathbf{x}_{\text{new}} = \mathbf{x}_{\text{old}} + \lambda\delta\mathbf{x}, \ 0 < \lambda < 1, \tag{38}$$

where $\delta\mathbf{x}$ is the same as given by Eq. 35. The routine first checks whether the value of $\mathbf{x}_{\text{new}}$ obtained with $\lambda = 1$ decreases the value of $f(\mathbf{x})$. If it occurs the algorithm goes to the next step, otherwise it tries using the values that fulfill $0 < \lambda < 1$. If the new value of $\mathbf{x}_{\text{new}}$ for some value of λ leads to a lower value of $f(\mathbf{x})$ then this new estimate of $\mathbf{x}_{\text{new}}$ is chosen. This procedure is referred to as backtracking. The technical details on the procedure of choice for λ are explained in Dennis and Schnabel (1983) and Press et al. (1992), and are outside the scope of the present paper.

4 A Note on Parameter Stability

4.1 Eddy-Covariance Measurements

The test of the calculation presented in this note has been carried out over a biomass crop (Cardoon, Cynara cardunculus L.) that demonstrated a great potential as a renewable energy source in the Mediterranean region (see Raccuia and Melilli 2007, among others). The crop was seeded on November 2009 in an experimental farm in Rutigliano southern Italy, 40°59′N,

Table 1 Input parameters directly calculated from high-frequency EC raw data

Input parameter	April 5 2010: 1100–1200 local time	April 7 2010: 1300–1400 local time
$\sigma_{q'}$ (g m^{-3})	0.455994	0.411163
$\sigma_{c'}$ (mg m^{-3})	4.544450	5.182580
$\langle w'q' \rangle$ (g m^{-2} s^{-1})	0.062700	0.033140
$\langle w'c' \rangle$ (mg m^{-2} s^{-1})	−0.712862	−0.472108
$\rho^{\text{obs}}_{q',c'}$	−0.922292	−0.881017
W (mg g^{-1})	−24.558131	−37.158598

Table 2 Output parameters resulting from the *newt* routine run

Output parameter	April 5 2010: 1100–1200 local time	April 7 2010: 1300–1400 local time
$\sigma_{c'_\text{p}}$ (mg m^{-3})	3.951510	5.230500
$\rho_{c'_\text{p},c'_\text{r}}$	−0.724706	−0.757626
$\langle w'q'_\text{e} \rangle / \langle wq_\text{t} \rangle$	1.466940	1.573370
$\langle w'q'_\text{e} \rangle$ (g m^{-2} s^{-1})	0.037284	0.020262
$\langle w'q'_\text{t} \rangle$ (g m^{-2} s^{-1})	0.025416	0.012878
$\langle w'c'_\text{r} \rangle$ (mg m^{-2} s^{-1})	−0.088690	0.004381
$\langle w'c'_\text{p} \rangle$ (mg m^{-2} s^{-1})	−0.624172	−0.476489

17°01′E, altitude 147 m a.s.l. The 2-ha surface cardoon field was irrigated only by 20 mm of water to facilitate emergence and settlement. For the remaining growing season (up to August 2010) only precipitation supplied water to the crop.

Fluxes of energy (sensible heat and latent heat), CO_2 and H_2O were measured using a three-dimensional sonic anemometer (USA-1, Metek GmbH, Germany) positioned at 1 m above the canopy. Atmospheric CO_2 and water vapour concentrations were measured with a fast-responding open-path infrared gas analyzer (IRGA, LI-7500, Li-COR Inc., Lincoln NE, USA). The sonic anemometer was mounted to ensure complete exposure in all directions. The input parameters refer to EC data obtained on April 5 2010, from 1100 to 1200 local time, and on April 7 2010, from 1300 to 1400 local time (see Table 1). At that moment the crop partially covered the soil (about 80 %) and was 0.70 m in height. All fluxes and variances are calculated with time averaging over an interval of 1 h. W was evaluated by using Eq. 39 below. In Table 2 the resulting output parameters are reported.

We decided to report several digits in the value of the algorithm inputs because, as shown in the next sections, a slight change in their value can lead to a condition without physical solution. For this reason we retained all the digits shown in Table 1 and then we explicitly study the sensitivity error with respect to the W and CO_2 flux $\langle w'c' \rangle$ uncertainties. When reporting the numerical results in Table 2, we maintain several digits in order to permit a precise check of our results compared with other solution algorithms. Of course one should always remember that the measurements and the propagated error are obviously much larger than the value implied by the number of digits reported.

As described before, the *newt* algorithm iterates the estimates solution in the plane $(\sigma_{c'_\text{p}}, \rho_{c'_\text{p},c'_\text{r}})$. These iterations are shown by the red points in Fig. 1, which also shows the loci of points fulfilling Eqs. 22 (blue points) and 29 (black points), separately. The solution of

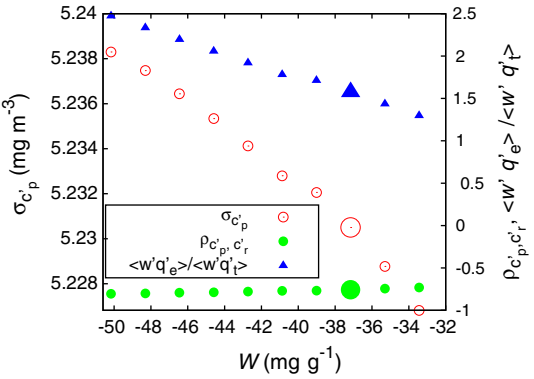

Fig. 2 Elaboration of the EC data obtained on April 7 2010 from 1300 to 1400, varying the W parameter. The threshold value W_0 value equals -14.24 mg g^{-1}

the system of equations we are looking for are the intersection of the blue and black curves. We see that the "trajectory" followed by the *newt* iterations is quickly reached after only five iterations.

4.2 Water-Use Efficiency

Following SS08, water-use efficiency W (mg g^{-1}) can be estimated as

$$W = 0.7\frac{\overline{c}_s - \overline{c}_i}{\overline{q}_s - \overline{q}_i} \leq 0 \tag{39}$$

where the coefficient 0.7 accounts for the differences in diffusion and convection between water vapour and carbon dioxide through the stomatal aperture, and the subscripts s and i relate to surface and interstomatal values, respectively, of q and c. In Appendix A of SS08, W was calculated with an inter-stomatal carbon concentration equal to 0.44 times the within-canopy carbon concentration, following Kim et al. (2006). The relationship between intra-stomatal and within-canopy CO_2 concentrations was experimentally demonstrated, but with a large standard error (up to 30 % as reported in Bacon, 2004). Concerning the internal concentration of q, SS08 suggest to estimate it on the basis of 100 % relative humidity at foliage temperature (T_L), where the last is approximated to be within ± 2°C of the measured air temperature (T_A), providing some flexibility for W.

In relation to the W range obtained from this flexibility, there is an important point that deserves some discussion. We have the "physical" condition that

$$|W| = \frac{|\langle w'c'_p\rangle|}{|\langle w'q'_t\rangle|} \geq \frac{|\langle w'c'_p\rangle|}{|\langle w'q'\rangle|} \geq \frac{|\langle w'c'\rangle|}{|\langle w'q'\rangle|}, \tag{40}$$

which, being $W \leq 0$ and $\langle w'c'_p\rangle \leq 0$, means

$$W \leq \frac{\langle w'c'\rangle}{\langle w'q'\rangle} \equiv W_0. \tag{41}$$

This implies that for $W > W_0$ no "physical" admissible solution exists. Consequently, it could be possible that some values in the W range do not obey the constraint defined in Eq. 41.

In Fig. 2 the value of the ratio between evaporated and transpirated water fluxes as a function of W is reported. The larger central point refers to the value of W obtained from

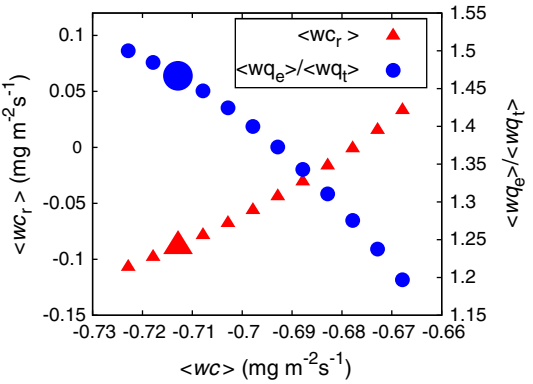

Fig. 3 Elaboration of the EC data obtained on April 5 2010 from 1100 to 1200 local time, varying the $\langle w'c' \rangle$ parameter in a range of $\pm 10\,\%$. Results lead to a remarkable effect on the change of the sign of $\langle w'c'_r \rangle$ turning a non-physical solution into an acceptable one. The change in the evaporation/transpiration ratio as a function of $\langle w'c' \rangle$ was also reported

the experimental measurements with $T_L = T_A$, while the others span in the range defined as $T_L = T_A \pm 2°C$.

4.3 Carbon Dioxide Flux

A last remark should be made on another reason that makes the solution of the SS08 algorithm unphysical. Very often in the data used, the solution should be discarded due to the fact that the algorithm leads to $\langle w'c'_r \rangle < 0$, which is of course a non-realistic condition. Nevertheless we note that the absolute value of $\langle w'c'_r \rangle < 0$ is very close to zero. Changing the W value in the range defined in Sect. 4.2 allows $\langle w'c'_r \rangle < 0$.

At this point, we vary the value of $\langle w'c' \rangle$ in the range of $\pm 10\,\%$, which is a reasonable estimate of the experimental error associated with these measurements. The results are reported in Fig. 3 where we show how the realistic condition can be recovered for a higher than measured value of $\langle w'c' \rangle$. We also plot the evaporation/transpiration ratio to show how the main result of the partition algorithm is influenced by the value of $\langle w'c' \rangle$. Thus we conclude that also during the period when the SS08 algorithm leads to an unphysical condition, a deeper analysis of the variability of the input measurements helps to extract the correct solution from the data.

5 Conclusions

This note shows that the method proposed in SS08 is reliable in giving good results in partitioning fluxes directly from high-frequency EC measurements only if it is used with some precautions. First of all one branch of solution can be neglected thanks to the Descartes' rule. Here we stress the fact that Eq. 21, with both values of the sign, may lead to more than one solution. As is apparent in Fig. 1, for the choice $+$, there are two $\sigma_{c'_p}$ values fulfilling Eq. 29 at fixed $\rho_{c'_p,c'_r}$. From a numerical point of view we think that our approach, based on Newton's method in two dimensions, is much faster, and consequently more applicable to a large dataset, if compared with the approach based on the substitution proposed by SS08.

In any case, we wish to stress the extreme instability of the results with respect to the estimated value of W. The parameter W is crucial for the calculations presented in SS08 and it is sufficient to allow the value of W to vary in the range given by its experimental uncertainty to ensure the system given by Eqs. 22 and 29 is not solvable.

For these reasons, we suggest to take into account the results reported in this note when the SS08 method is applied in flux partitioning derived from high-frequency EC measurements, or simply for further research aimed at improving the method.

Acknowledgments This work has been supported by the two Italian projects Biodati (D.M. 15421 4/07/2011) and CLIMESCO (FISR D.D. no. 285 20/02/2006). The experimental measurements are courtesy given by the National Research Project "Optimization of existing bioenergy chains for economic and environmental sustainability" (BIOSEA), funded by the Ministry of Agriculture, Food and Forestry Policies (MiPAAF), Italy. LP thanks the SSD PESCA and the RITMARE Italian Research Ministry (MIUR) Projects. DV has been supported by EC project ICOS-INWIRE (FPT/2007-2013, grant agreement n. 313169). We thank G. Lacorata for the suggestion of using the absolute value of Δ in the numerical calculations.

References

Bacon M (2004) Water use efficiency in plant biology. Blackwell, Oxford, 327 pp

Baldocchi D, Falge E, Gu L, Olson R, Hollinger D, Running S, Anthoni P, Bernhofer C, Davis K, Evans R, Fuentes J, Goldstein A, Katul G, Law B, Lee X, Malhi Y, Meyers T, Munger W, Oechel W, Paw KT, Pilegaard K, Schmid HP, Valentini R, Verma S, Vesala T, Wilson K, Wofsy S (2001) FLUXNET: A new tool to study the temporal and spatial variability of ecosystem-scale carbon dioxide, water vapor, and energy flux densities. Bull Am Meteorol Soc 82:2415–2434

Bink NJ, Meesters AGCA (1997) Comment on Estimation of surface heat and momentum fluxes using the flux variance method above uniform and non-uniform terrain by Katul et al. 1995. Boundary-Layer Meteorol 84:497–502

Dennis JE, Schnabel RB (1983), Numerical methods for unconstrained optimization and nonlinear equations. Prentice-Hall, Englewood Cliffs, 378 pp (Reprinted as Classics in applied mathematics, vol 16, 1996)

Katul GG, Goltz SM, Hsieh CI, Cheng Y, Mowry F, Sigmon J (1995) Estimation of surface heat and momentum fluxes using the fluxvariance method above uniform and non-uniform terrain. Boundary-Layer Meteorol 74:237–260

Katul GG, Finkelstein PL, Clarke JF, Ellelstad TG (1996) An investigation of the conditional sampling method used to estimate fluxes of active, reactive and passive scalars. J Appl Meteorol 35:1835–1845

Kim SH, Sicher RC, Bae H, Gitz DC, Baker JT, Timlin DJ, Reddy VR (2006) Canopy photosynthesis, evapotranspiration, leaf nitrogen, and transcription profiles of maize in response to CO2 enrichment. Glob Change Biol 12:588–600

Lasslop G, Reichstein M, Papale D, Richardson AD, Arneth A, Barr A, Stoy P, Wohlfahrt G (2010) Separation of net ecosystem exchange into assimilation and respiration using a light response curve approach: critical issues and global evaluation. Glob Change Biol 16:187–208

Press WH, Teukolsky SA, Vetterling WT, Flannery BP (1992) Numerical recipes in C: the art of scientific computing. Cambridge University Press, Cambridge, 925 pp

Raccuia SA, Melilli MG (2007) Biomass and grain oil yields in *Cynara cardunculus* L. genotypes grown in a Mediterranean environment. Field Crop Res 101:187–197

Reichstein M, Falge E, Baldocchi D, Papale D, Aubinet M, Berbigier P, Bernhofer C, Buchmann N, Gilmanov T, Granier A, Grüunwald T, Havránková K, Ilvesniemi H, Janous D, Knohl A, Laurila T, Lohila A, Loustau D, Matteucci G, Meyers T, Miglietta F, Ourcival J-M, Pumpanen J, Rambal S, Rotenberg E, Sanz M, Tenhunen J, Seufert G, Vaccari F, Vesala T, Yakir D, Valentini R (2005) On the separation of net ecosystem exchange into assimilation and ecosystem respiration: review and improved algorithm. Glob Change Biol 11:1424–1439

Reichstein M, Stoy PC, Desai AR, Lasslop G, Richardson AD (2012) Partitioning of net fluxes. In: Aubinet M et al. (eds) Eddy covariance: a practical guide to measurement and data analysis, Chap 9. Springer Atmospheric Sciences, Berlin, pp 263–289

Scanlon TM, Kustas WP (2010) Partitioning carbon dioxide and water vapor fluxes using correlation analysis. Agric For Meteorol 150:89–99

Scanlon TM, Sahu P (2008) On the correlation structure of water vapor and carbon dioxide in the atmospheric surface layer: a basis for flux partitioning. Water Resour Res 44:W10418